

Mass distribution exponents for growing trees

F. David¹, P. Di Francesco¹, E. Guitter¹ and T. Jonsson²

¹*Service de Physique Théorique, CEA/DSM/SPhT
Unité de recherche associée au CNRS
CEA/Saclay
91191 Gif sur Yvette Cedex,
France*

²*Science Institute,
University of Iceland,
Dunhaga 3, 107 Reykjavik,
Iceland*

francois.david@cea.fr
philippe.di-francesco@cea.fr
emmanuel.gutter@cea.fr
thjons@raunvis.hi.is

Abstract

We investigate the statistics of trees grown from some initial tree by attaching links to preexisting vertices, with attachment probabilities depending only on the valence of these vertices. We consider the asymptotic mass distribution that measures the repartition of the mass of large trees between their different subtrees. This distribution is shown to be a broad distribution and we derive explicit expressions for scaling exponents that characterize its behavior when one subtree is much smaller than the others. We show in particular the existence of various regimes with different values of these mass distribution exponents. Our results are corroborated by a number of exact solutions for particular solvable cases, as well as by numerical simulations.

1. Introduction

Random trees arise in many branches of science, ranging from the social sciences through biology, physics and computer science to pure mathematics. In physics, random trees often occur in the context of statistical mechanics or quantum field theory where the weight or probability of a tree is given by a local function, e.g. a Boltzmann factor with an energy which depends only on the valence of individual vertices but not on global features of the tree. A motivation for study of such trees comes for instance from results in the theory of random surfaces which behave like trees in some cases, see [1]. Another motivation concerns the study of two-dimensional quantum gravity by use of so-called causal tessellations [2], directly expressible in terms of random walks or of trees [3].

Another large class of random trees arises in *growth processes* where a tree evolves in time by adding new vertices which attach themselves by a link to one of the vertices of a preexisting tree according to some stochastic rules, with local attachment probabilities. A possible realization is a tree-like molecule (branched polymer) growing in a solution with an abundance of monomers. In many important real world cases one can observe the structure of the growing tree but only guess the rules which govern the growth (social networks, the internet, citation networks etc.). For a review of this topic, see [4].

Most tree models in statistical mechanics with a local energy function fall into one universality class, called *generic random trees*, with susceptibility exponent $\gamma = 1/2$, intrinsic Hausdorff dimension 2 and spectral dimension $4/3$ [5]. This universality class corresponds also to the mean field theory of branched polymers. If we look at a generic infinite tree, then with probability 1 there is a unique infinite non-backtracking path [6]. A rooted generic tree can therefore be viewed as an infinite half-line with finite trees growing out of it and these finite outgrowths have a well-understood distribution. This means that if we sit at a vertex of a generic random tree, almost all the vertices of the tree are to be found in the direction of one of the links emanating from this vertex.

There do not seem to be any local growth rules for a tree which produce generic trees. In this paper we study the structure of growing trees and focus on how they differ from generic trees. Taking binary planar trees with a root of valence one as an example we can ask what proportion of the vertices sits on the right hand side of the tree and what proportion on the left. For a generic tree almost all the vertices are on one side. We will see that with local growth rules, in the limit of infinite trees, we get a continuous distribution for the proportion of vertices sitting on each side. We will refer to this distribution as the *mass distribution*. This quantity is one of the simplest geometrical characterizations of the geometry of the random trees and gives a first glimpse at their fractal structure. It might also be of practical use, for instance when applied to binary search trees, to improve algorithmic efficiency by anticipating the structure of stored data. The aim of this paper is an investigation of this mass distribution, in particular via the derivation of scaling exponents characterizing its behavior when one side of the tree is much smaller than the other. Those exponents turn out to depend precisely on the underlying growth dynamics and also on the initial condition of the growth process.

As long as we are interested only in global properties such as the mass distribution,

the growth process reduces to a model of evolution of populations which belongs to the class of so-called generalized Pólya urn problems [7]. These problems have been analyzed using continuous time branching processes [8-10] and we believe that the mass distribution exponents can in principle be deduced using those methods. However, we find it illuminating to study the model directly using discrete time and elementary methods.

We first consider growing binary trees which are characterized by a single parameter x given by the ratio between the probabilities that a new vertex attaches itself to an old vertex of valence 1 or of valence 2. For a certain value of x the model can be mapped onto a simple model of reinforced random walk which is exactly solvable. When starting from the tree consisting of a single link, one finds a uniform mass distribution, i.e. the probability that a fraction u of the total mass sits on the left is independent of u . More generally, this distribution is given by a Beta law that depends on the initial tree that we start the growth process from. For other, arbitrary values of the parameter x , we show how to calculate the mass distribution exponents exactly by scaling arguments. Again, these exponents depend strongly on the initial condition.

In the second half of the paper these results are generalized to the case of growing trees with vertices of a uniformly bounded valence. Both for binary and the more general multinary trees numerical experiments have been carried out and are in excellent agreement with the scaling results.

2. Growth of binary trees

2.1. Definition of the model

The model that we will study consists of growing binary trees from some finite initial binary tree \mathcal{T}^0 by successive addition of links. As usual, the binary trees are rooted at some *root edge* and planar, which allows to distinguish left and right descendants at each vertex. One may alternatively think of the trees as drawn on top of some underlying infinite binary Cayley tree with a unique leaf connected to the *root edge* (see figure 1). The growing of a new link takes place at uni- or bi-valent vertices of the existing tree only, with two choices (left or right descendant) in the first case and a unique choice (the descendant not already occupied) in the second case. At each step, the choice of the vertex to which we attach the new link is made with a probability that depends on its valence i ($i = 1, 2$) and chosen to be proportional to w_1 for univalent vertices and w_2 for bivalent ones. More precisely, if we denote by n_i , $i = 1, 2, 3$ the total number of i -valent vertices on the growing tree at a given step, the probability to attach the new link to a given i -valent vertex reads $w_i/(n_1w_1 + n_2w_2)$ for $i = 1, 2$. Note that the process depends only on the quantity w_1/w_2 . Once the choice of attachment vertex is made, the precise choice of link to add is then unambiguous if $i = 2$ and uniformly distributed on the left and right descendants if $i = 1$.

In the following, we will concentrate on *global properties* of the growing tree, such as its total numbers n_i of i -valent vertices. The above growing process induces a Markovian evolution for $n_i(t)$ as functions of a *discrete time* t equal to the number of added links,

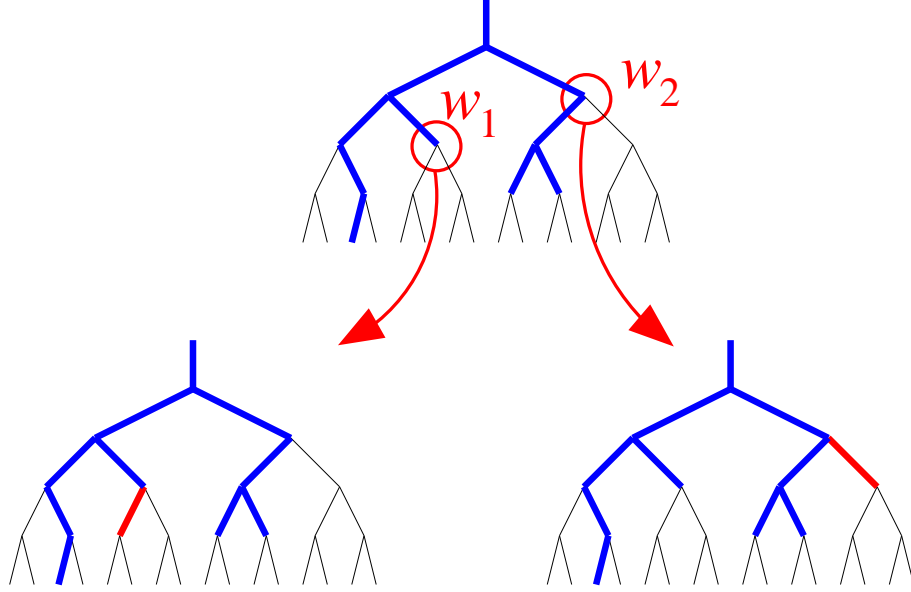


Fig. 1: A sample binary tree (top, thick lines) grown on top of an underlying infinite binary Cayley tree (thin lines) by attaching a new link either at a univalent vertex (bottom left) or at a bivalent one (bottom right). The choice of the attachment vertex is made with probability weights w_i depending only on its valence $i = 1$ or 2 . When $i = 1$, the new link is chosen among the two possible descendants with equal probabilities.

starting from $n_i(0) \equiv n_i^0$, the numbers of i -valent vertices on \mathcal{T}^0 . We have the following evolution rules:

$$\begin{aligned}
 &\text{with probability } \frac{n_1(t)w_1}{n_1(t)w_1 + n_2(t)w_2}, & \begin{cases} n_1(t+1) &= n_1(t) \\ n_2(t+1) &= n_2(t) + 1 \\ n_3(t+1) &= n_3(t) \end{cases} \\
 &\text{with probability } \frac{n_2(t)w_2}{n_1(t)w_1 + n_2(t)w_2}, & \begin{cases} n_1(t+1) &= n_1(t) + 1 \\ n_2(t+1) &= n_2(t) - 1 \\ n_3(t+1) &= n_3(t) + 1 \end{cases}
 \end{aligned} \tag{2.1}$$

These rules are a particular realization of so-called generalized Pólya urns with three types of “balls” taken out of a single urn. The problem can thus be studied by continuous time branching processes (see [8]) but we prefer to present here some heuristic but more direct arguments. The rules (2.1) translate into a *master equation* for the probability $p(n_1, n_2, n_3; t)$ that there be n_i i -valent vertices in the growing tree at time t :

$$\begin{aligned}
 p(n_1, n_2, n_3; t+1) &= \frac{n_1 w_1}{n_1 w_1 + (n_2 - 1) w_2} p(n_1, n_2 - 1, n_3; t) \\
 &+ \frac{(n_2 + 1) w_2}{(n_1 - 1) w_1 + (n_2 + 1) w_2} p(n_1 - 1, n_2 + 1, n_3 - 1; t) .
 \end{aligned} \tag{2.2}$$

This, together with the initial conditions $p(n_1, n_2, n_3, 0) = \prod_{i=1}^3 \delta_{n_i, n_i^0}$, determines $p(n_1, n_2, n_3; t)$ completely.

Defining the total *mass* T of the evolving tree as its total number of edges (including the root edge), we have clearly the relation $T = t + T^0$, where T^0 is the mass of the initial tree \mathcal{T}^0 . Moreover, we have the standard relations for binary trees:

$$T = n_1 + n_2 + n_3 = 2n_1 + n_2 - 1 . \quad (2.3)$$

We may therefore write

$$p(n_1, n_2, n_3; t) = \delta_{n_2, t+T^0+1-2n_1} \delta_{n_3, n_1-1} p(n_1; t) . \quad (2.4)$$

Hence, the problem reduces to finding a function of two variables only.

The proportions $n_i(t)/T$ of the total mass corresponding to edges antecedent of i -valent vertices provide a first set of interesting quantities. As we shall see in the next section, these proportions tend asymptotically at large t to fixed values depending on w_1/w_2 only and *not* on the initial condition. Moreover, these values may be computed exactly via a simple mean-field argument.

As mentioned in the introduction, another interesting quantity that characterizes the geometry of the growing tree is given by the repartition of the total mass between *the left and the right of the root edge*. Defining the left and right masses T_L and T_R as the total number of edges in the left and right descending subtrees of the root edge (with $T_L + T_R = T - 1$), we shall be interested in the asymptotic proportions $u_L = T_L/(T - 1)$ and $u_R = T_R/(T - 1)$ at large t (with $u_R = 1 - u_L$). The corresponding limiting law $P(u_L, u_R)$ is quite subtle and cannot be obtained by mean-field arguments. As we shall see below, the proportions u_L and u_R are not peaked to fixed values but are instead characterized by a broad asymptotic probability distribution $P(u_L, u_R)$ on $[0, 1]$, which moreover depends strongly on the initial conditions. The main subject of this paper is an investigation of this limiting law and in particular the derivation of exponents that characterize it.

2.2. Mean-field results

The mean-field approach consists in assuming that the proportions of mass under study are peaked at large t around fixed values and in neglecting fluctuations around those. As we shall see, this gives a fully consistent result in the case of the proportions n_i/T above, while it gives no information on the left and right proportions u_L and u_R .

Multiplying both sides of eq. (2.2) by n_1 , (resp. n_2 , n_3) and summing over all n 's at fixed t , we get

$$\begin{aligned} \langle n_1 \rangle_{t+1} &= \langle n_1 \rangle_t + \left\langle \frac{n_2 w_2}{n_1 w_1 + n_2 w_2} \right\rangle_t \\ \langle n_2 \rangle_{t+1} &= \langle n_2 \rangle_t + \left\langle \frac{n_1 w_1 - n_2 w_2}{n_1 w_1 + n_2 w_2} \right\rangle_t \\ \langle n_3 \rangle_{t+1} &= \langle n_3 \rangle_t + \left\langle \frac{n_2 w_2}{n_1 w_1 + n_2 w_2} \right\rangle_t \end{aligned} \quad (2.5)$$

Here, the notation $\langle \dots \rangle_t$ stands for the average over all possible growths of the initial tree \mathcal{T}^0 by adding t links. The mean-field hypothesis allows to substitute $n_i \rightarrow \alpha_i t$ within averages in (2.5), with constants α_i to be determined. This substitution immediately yields

$$\alpha_1 = \alpha_3 = \frac{\alpha_2 w_2}{\alpha_1 w_1 + \alpha_2 w_2} \quad \alpha_2 = \frac{\alpha_1 w_1 - \alpha_2 w_2}{\alpha_1 w_1 + \alpha_2 w_2} \quad (2.6)$$

which fixes

$$\alpha_1 = \alpha_3 = \frac{2x}{3x + \sqrt{x(8+x)}} \quad \alpha_2 = \frac{2}{2+x + \sqrt{x(8+x)}} \quad (2.7)$$

where

$$x \equiv \frac{2w_2}{w_1} . \quad (2.8)$$

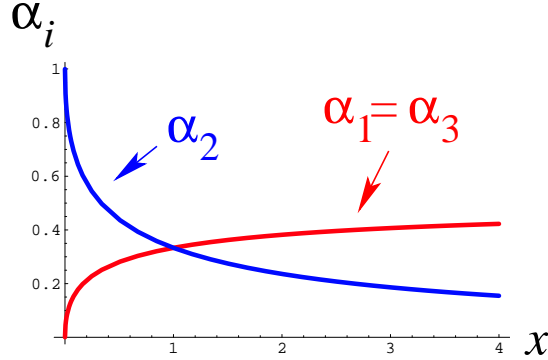


Fig. 2: The limiting proportions $\alpha_i \sim n_i/t$ at large t as functions of the ratio $x = 2w_2/w_1$, with values (2.7) predicted by a mean field argument.

These values are plotted in fig.2. Note that we have the relations $\alpha_1 + \alpha_2 + \alpha_3 = 2\alpha_1 + \alpha_2 = 1$ in agreement with eq. (2.3).

To check this mean-field result, we may use the master equation (2.2) to estimate the asymptotics of $p(n_1, t)$ in (2.4). Performing the substitution (2.4) into eq. (2.2), we get

$$\begin{aligned} p(n_1; t+1) &= \frac{n_1 w_1}{n_1 w_1 + (t + T^0 + 1 - 2n_1)w_2} p(n_1; t) \\ &+ \frac{(t + T^0 + 3 - 2n_1)w_2}{(n_1 - 1)w_1 + (t + T^0 + 3 - 2n_1)w_2} p(n_1 - 1; t) \end{aligned} \quad (2.9)$$

At large t , we assume that the solution takes the asymptotic form

$$p(n_1; t) \sim \frac{1}{\sqrt{t}} f\left(\frac{n_1}{\sqrt{t}} - \alpha_1 \sqrt{t}\right) \quad (2.10)$$

for some function $f(z)$ and some parameter α_1 to be determined. Substituting this form into eq. (2.9) and expanding in $1/\sqrt{t}$ at large t , we get at leading order the consistency relation

$$\frac{w_1}{w_2} = \frac{(1 - \alpha_1)(1 - 2\alpha_1)}{\alpha_1^2} \quad (2.11)$$

from which we recover the value α_1 of eq. (2.7), while the values of α_2 and α_3 follow from $\alpha_2 = 1 - 2\alpha_1$ and $\alpha_3 = \alpha_1$. At sub-leading order, we get a differential equation for $f(z)$:

$$(3 - 4\alpha_1)(f + z f') + \alpha_1(1 - \alpha_1)(1 - 2\alpha_1)f'' = 0 \quad (2.12)$$

from which we deduce that

$$f(z) \propto e^{-\frac{3-4\alpha_1}{2\alpha_1(1-\alpha_1)(1-2\alpha_1)}z^2} \quad (2.13)$$

As announced, the asymptotic distribution for n_1/t is peaked around the mean value α_1 . More precisely, it is Gaussian with a width of order $1/\sqrt{t}$, hence tends to $\delta(n_1/t - \alpha_1)$ when $t \rightarrow \infty$.

It is interesting to apply the same mean-field approach to the case of the left-right repartition of the mass in the growing tree. The above Markov process must now be refined so as to keep track of the left (L) and right (R) numbers of uni- and bi-valent vertices $n_{i,A}$, $i = 1, 2$ and $A = L, R$. The masses on the left and right of the root edge are then simply expressed as $T_L = 2n_{1,L} + n_{2,L} - 1$ and $T_R = 2n_{1,R} + n_{2,R} - 1$. Here and throughout the paper, we use the convention that $n_{1,L} = 0$, $n_{2,L} = 1$ if the left subtree is empty, and similarly for the right subtree. If we now assume the existence of limiting proportions $n_{i,A}/t \rightarrow \eta_{i,A}$ at large t , we get the mean-field equations

$$\begin{aligned} \eta_{1,L} &= w_2 \eta_{2,L} / \Sigma \\ \eta_{2,L} &= (w_1 \eta_{1,L} - w_2 \eta_{2,L}) / \Sigma \\ \eta_{1,R} &= w_2 \eta_{2,R} / \Sigma \\ \eta_{2,R} &= (w_1 \eta_{1,R} - w_2 \eta_{2,R}) / \Sigma \end{aligned} \quad (2.14)$$

where $\Sigma = \Sigma_L + \Sigma_R$ and $\Sigma_A = w_1 \eta_{1,A} + w_2 \eta_{2,A}$. We introduce the quantities $u_A \equiv 2\eta_{1,A} + \eta_{2,A}$, which are nothing but the asymptotic proportions of the total mass lying on the left and right of the root edge. From eq. (2.14), we deduce that $u_A = \Sigma_A / \Sigma$, henceforth $u_L + u_R = 1$ as it should. Introducing $\alpha_{i,A} = \eta_{i,A} / u_A$, which are the proportions of uni- and bi-valent vertices *within* the left, resp. right subtree, eqs. (2.14) decouple into two sets of equations

$$\begin{cases} \alpha_{1,L} &= \alpha_{2,L} w_2 / (\alpha_{1,L} w_1 + \alpha_{2,L} w_2) \\ \alpha_{2,L} &= (\alpha_{1,L} w_1 - \alpha_{2,L} w_2) / (\alpha_{1,L} w_1 + \alpha_{2,L} w_2) \\ \alpha_{1,R} &= \alpha_{2,R} w_2 / (\alpha_{1,R} w_1 + \alpha_{2,R} w_2) \\ \alpha_{2,R} &= (\alpha_{1,R} w_1 - \alpha_{2,R} w_2) / (\alpha_{1,R} w_1 + \alpha_{2,R} w_2) \end{cases} \quad (2.15)$$

which are identical to the mean field equation (2.6). We deduce that $\alpha_i^L = \alpha_i^R = \alpha_i$ of eq. (2.7) while u_L and u_R remain *undetermined*. In other words, the relative proportions of uni- and bi-valent vertices within each subtree tend asymptotically to the same mean field values as in the whole tree, but the distribution $P(u_L, u_R)$ is not peaked to particular values. We expect instead a broad distribution in the whole interval $[0, 1]$. This property will be illustrated in the next section in a particular case.

2.3. A solvable case

A particularly interesting case corresponds to growing the binary trees by adding links chosen *uniformly at random* among all possible available positions. This amounts to taking $w_1 = 2w_2$ as there are twice as many available descendants at univalent vertices as there are at bivalent ones. This corresponds to $x = 1$ in (2.8). For simplicity, we take $w_1 = 2$ and $w_2 = 1$ so that $w_1 n_1 + w_2 n_2 = 2n_1 + n_2$ directly counts the number of available positions for the addition of a link. This number is nothing but the mass T of the tree plus 1. Therefore, the evolution process no longer depends on n_1 and n_2 individually, but instead depends on the total mass T only.

Turning to left and right proportions, we need only keep track of the masses T_L and T_R of the right and left subtree (with $T_L + T_R = T - 1$). The induced evolution process consists at each step in increasing the mass by one on the left with probability $(T_L + 1)/(T + 1)$ and on the right with probability $(T_R + 1)/(T + 1)$. This process is known as the reinforced random walk (RRW) in which a walker goes to the left (resp. to the right) with a probability proportional to the number of times he has already stepped in this direction. For a review on reinforced processes, see for instance [7]. We may easily write a master equation for the probability $p(T_L, T_R; t)$ to have masses T_L and T_R at time t (with $T = t + T^0$):

$$p(T_L, T_R; t + 1) = \frac{T_L}{t + T^0 + 1} p(T_L - 1, T_R; t) + \frac{T_R}{t + T^0 + 1} p(T_L, T_R - 1; t) \quad (2.16)$$

where $T^0 = T_L^0 + T_R^0 + 1$ and T_L^0 and T_R^0 are the initial left and right masses. Together with the initial condition $p(T_L, T_R, 0) = \delta_{T_L, T_L^0} \delta_{T_R, T_R^0}$, this fixes the solution to be

$$p(T_L, T_R; t) = \frac{\binom{T_L}{T_L^0} \binom{T_R}{T_R^0}}{\binom{t+T^0}{T^0}} \delta_{T_L+T_R+1, t+T^0} \quad (2.17)$$

In particular, when we start from an initial tree \mathcal{T}^0 consisting of the root edge alone, we have $T^0 = 1$, $T_L^0 = T_R^0 = 0$ and therefore $p(T_L, T_R; t) = \delta_{T_L+T_R, t}/(t + 1)$. Hence, all the values $T_L = 0, 1, \dots, t$ are *equiprobable*. This is a well-known feature of the RRW.

At large t and for arbitrary initial conditions, we may extract from eq. (2.17) the asymptotic law for the probability distribution of the left and right mass proportions u_L and u_R by writing $P(u_L, u_R) = \lim_{t \rightarrow \infty} t^2 p(u_L(t + T^0 - 1), u_R(t + T^0 - 1); t)$. We get explicitly

$$P(u_L, u_R) = \frac{(T_L^0 + T_R^0 + 1)!}{T_L^0! T_R^0!} u_L^{T_L^0} u_R^{T_R^0} \delta(u_L + u_R - 1) \quad (2.18)$$

We thus get a simple Beta law with exponents T_L^0 and T_R^0 , the left and right masses of the initial tree.

At this stage, a few remarks are in order. First, as announced, the distribution $P(u_L, u_R)$ is supported over the whole interval $[0, 1]$. Next, it explicitly depends on the initial condition. However, we note that this dependence is only through the initial masses and does not involve the precise shape of the initial left or right trees. In view of this discussion, we define the *left and right exponents* β_L and β_R through

$$\begin{aligned} P(u_L, u_R) &\sim u_L^{\beta_L} && \text{when } u_L \rightarrow 0 \\ P(u_L, u_R) &\sim u_R^{\beta_R} && \text{when } u_R \rightarrow 0 \end{aligned} \tag{2.19}$$

Here we have $\beta_L = T_L^0$ and $\beta_R = T_R^0$, and, as the distribution is a Beta law, the left and right exponents characterize it completely. Note that the left exponent β_L depends only on the left initial condition and not on the right one and vice-versa. As we will see later, this property will remain true for arbitrary values of w_1 and w_2 .

3. Mass distribution exponents

In this section, we derive the left and right exponents β_L and β_R defined in (2.19) for the general case of arbitrary w_1 and w_2 and for arbitrary initial conditions.

3.1. Results

Before we proceed to the actual derivation of the exponents, let us display and discuss the corresponding formula that we obtain. We have the simple expression

$$\begin{aligned} \beta_L &= -1 + \frac{1}{\alpha_1 w_1 + \alpha_2 w_2} \min_{\mathcal{T} \supset \mathcal{T}_L^0} \{w_1 n_1(\mathcal{T}) + w_2 n_2(\mathcal{T})\} \\ \beta_R &= -1 + \frac{1}{\alpha_1 w_1 + \alpha_2 w_2} \min_{\mathcal{T} \supset \mathcal{T}_R^0} \{w_1 n_1(\mathcal{T}) + w_2 n_2(\mathcal{T})\} \end{aligned} \tag{3.1}$$

where α_1 and α_2 are the limiting proportions given by eq. (2.7) and where the minimum is taken over all binary trees \mathcal{T} containing the left (resp. right) initial subtree \mathcal{T}_L^0 (resp. \mathcal{T}_R^0), with $n_i(\mathcal{T})$ being the number of i -valent vertices in \mathcal{T} . In the above formula, we use again the convention that whenever \mathcal{T} is empty, we have $n_1(\mathcal{T}) = 0$ and $n_2(\mathcal{T}) = 1$. The minimum may be explicitly evaluated and depends on the relative values of w_1 and w_2 . Indeed, any binary tree \mathcal{T} containing, say \mathcal{T}_L^0 , may be obtained from \mathcal{T}_L^0 by the successive addition of a number of links. At each step, the quantity $n_1 w_1 + n_2 w_2$ either increases by $w_2 > 0$ if the link is added at a univalent vertex, or is shifted by $w_1 - w_2$ if it is added at a bivalent vertex. If $w_1 > w_2$, the quantity $n_1 w_1 + n_2 w_2$ may therefore only increase strictly and the minimum is attained for the initial state $\mathcal{T} = \mathcal{T}_L^0$, with value $w_1 n_{1,L}^0 + w_2 n_{2,L}^0$, where $n_{i,L}^0 \equiv n_i(\mathcal{T}_L^0)$. When $w_1 < w_2$, the minimum is obtained by saturating each bivalent vertex of \mathcal{T}_L^0 into a trivalent vertex and a uni-valent one. The

resulting tree \mathcal{T} has no more bivalent vertices and a number $n_{1,L}^0 + n_{2,L}^0$ of univalent ones. The associated minimum now reads $w_1(n_{1,L}^0 + n_{2,L}^0)$. We finally obtain the following explicit expression:

$$\beta_L = -1 + \frac{x + \sqrt{x(8+x)}}{8x} (4n_{1,L}^0 + (x+2 - |x-2|)n_{2,L}^0) \quad (3.2)$$

and a similar expression for the right exponent. As mentioned above, we use the convention that $n_{1,L}^0 = 0$ and $n_{2,L}^0 = 1$ if \mathcal{T}_L^0 is empty. Note that the left exponent only depends on the left initial subtree via its numbers $n_{i,L}^0$ of uni- and bi-valent vertices.

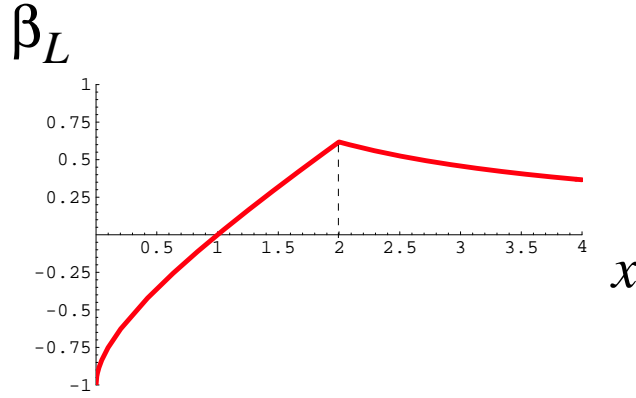


Fig. 3: Left mass distribution exponent β_L as a function of $x = 2w_2/w_1$ for an initial empty left subtree, with value given by (3.2) with $n_{1,L}^0 = 0$ and $n_{2,L}^0 = 1$. At $x = 1$, we see the value $\beta_L = 0$ of section 2.3. A change of regime takes place at $x = 2$, i.e. $w_1 = w_2$.

The exponent β_L is displayed in fig.3 for the simple case where we start from an empty left subtree.

A few remarks are in order. First we note that, as a first check of our formula, we recover when $x = 1$ the result $\beta_L = 2n_{1,L}^0 + n_{2,L}^0 - 1 = T_L^0$ of section 2.3. Two other particular values of x may be easily checked, namely $x \rightarrow 0$ and $x \rightarrow \infty$, as the corresponding limiting growth processes may be easily analyzed.

When $x \rightarrow 0$, we find that β_L tends to infinity unless $n_{1,L}^0 = 0$, which corresponds to an empty initial left subtree in which case $\beta_L = -1$. These results may be understood as follows. For $x \rightarrow 0$, i.e. $w_1 \gg w_2$, the trees that are built are extensions of the initial tree by polymer-like chains (without new branching) attached to the initial leaves. If at least one of the left or right initial subtrees is non-empty, the number of attachment points for the chains is $n_{1,L}^0$ on the left and $n_{1,R}^0$ on the right, with $n_{1,L}^0 + n_{1,R}^0 > 0$, hence at large t , we have

$$P(u_L, u_R) \rightarrow \delta(u_L - \frac{n_{1,L}^0}{n_{1,L}^0 + n_{1,R}^0}) \delta(u_R - \frac{n_{1,R}^0}{n_{1,L}^0 + n_{1,R}^0}) \quad (3.3)$$

If $n_{1,L}^0 = 0$, we have a delta peak at $u_L = 0$, which is consistent with the limiting value $\beta_L = -1$. If $n_{1,L}^0 > 0$, we have delta peak at a positive value of u_L , consistent with a limiting value $\beta_L = \infty$. Finally, when both initial subtrees are empty ($n_{1,L}^0 = n_{1,R}^0 = 0$), the first step consist in attaching a link to the root edge with probability $1/2$ on the left or on the right and one then grows a single chain on this side. We therefore have $P(u_L, u_R) = (\delta(u_L)\delta(u_R - 1) + \delta(u_L - 1)\delta(u_R))/2$, again consistent with $\beta_L = -1$.

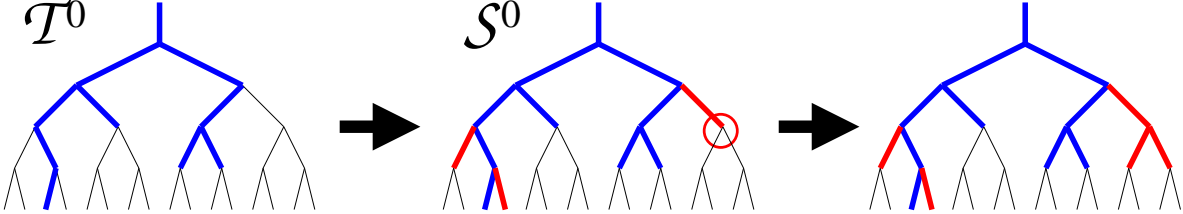


Fig. 4: A typical growth process at $x = \infty$ (from left to right). The process starts by first saturation all bivalent vertices of the initial tree \mathcal{T}^0 (left) into trivalent ones, resulting in a tree \mathcal{S}^0 (middle) with no more bivalent vertices. The growth then proceeds by a two-step elementary process which consist in adding the two descendant links to a leaf (circled) chosen uniformly among all leaves, and so on.

Another interesting case is the limit $x \rightarrow \infty$, i.e. $w_2 \gg w_1$. In this case, the growth process consists in first saturating all initial bivalent vertices into trivalent ones, resulting in a tree \mathcal{S}^0 without bivalent vertex and with left and right masses $S_A^0 = 2(n_{1,A}^0 + n_{2,A}^0) - 1$, $A = R, L$ (see fig.4). Again we use the convention that $n_{1,A}^0 = 0$, $n_{2,A}^0 = 1$ if the tree on side A is empty. Note that if we start from a configuration \mathcal{T}^0 reduced to the root edge, the first two steps of the growing process consist in adding to the root edge the two links that descend from it. We define for consistency \mathcal{S}^0 as this resulting tree, with $S_L^0 = S_R^0 = 1$. The growth then proceeds by a succession of two-step elementary processes that add at some existing leaf a *pair of links* on its left and right descendants. The choice of the leaf at which we attach the new pair is moreover uniform among all leaves. Remarkably, this two-step process with initial condition \mathcal{S}^0 is completely equivalent to the process of section 2.3 with $x = 1$, where we were choosing *single* descendants uniformly. This is due to the existence of a bijection between “saturated” binary trees without bivalent vertices and ordinary binary trees illustrated in fig.5, obtained by erasing the root edge and squeezing all pairs of descendants into single links. The left mass of the image of \mathcal{S}^0 under the above bijection reads $(S_L^0 - 1)/2 = n_{1,L}^0 + n_{2,L}^0 - 1$. From the results of section 2.3, we thus get for the left exponent the value $\beta_L = n_{1,L}^0 + n_{2,L}^0 - 1$, in agreement with (3.2) at $x \rightarrow \infty$.

Beyond the three solvable cases $x = 0, 1$ and ∞ above, we can deduce a number of qualitative results from our general formula (3.2). First, the distribution is not in general a Beta law. Indeed, this would require that the exponents for different initial conditions differ by integers, which is not the case for generic x . Second, if we start from the tree consisting of a single edge, the distribution can be maximal at $u_L = u_R = 1/2$

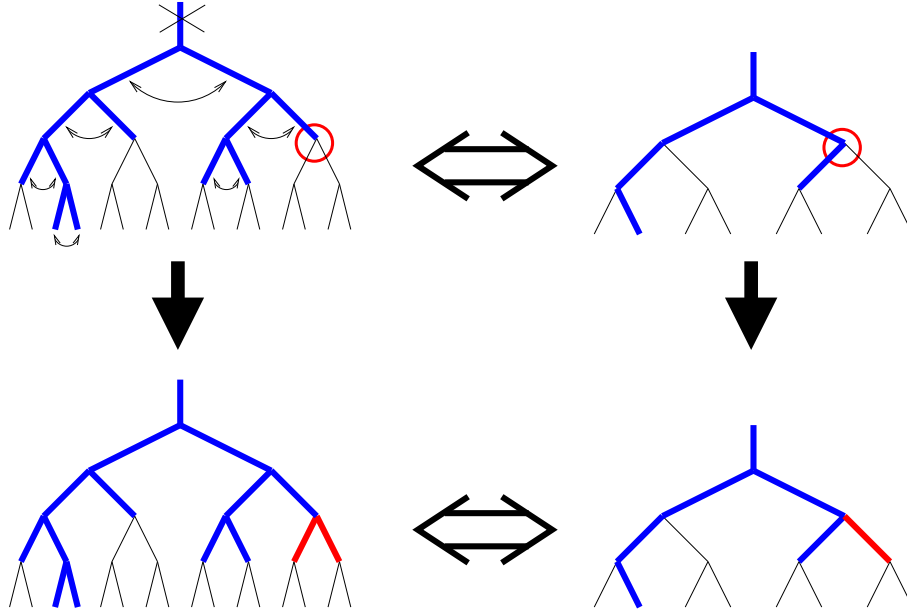


Fig. 5: The bijection between “saturated” binary trees (top left) without bivalent vertices and ordinary binary trees (top right), obtained by erasing the root edge and squeezing all pairs of descendants into single links. The $x = \infty$ growth process consisting in adding both descendants of a leaf chosen uniformly at random (bottom left) is bijectively mapped onto the $x = 1$ growth process where single links are added uniformly at random (bottom right).

for $x > 1$, or conversely, it can be maximal at $u_L = 0$ or $u_R = 0$ for $x < 1$. Third, we see a change of behavior of the model at $x = 2$ with a change of determination for the exponents which suggests the existence of a competition between different effective growth mechanisms. Finally, the fact that the exponent β_L increases with the size of the initial tree is a general feature of reinforced processes. Indeed, starting from a large tree amounts to impose a preferential value of the mass ratio, leading to a narrower distribution.

3.2. Large time behavior

In order to estimate the, say left mass distribution exponent β_L , we are led to consider growth processes in which the left subtree *remains finite* at large time t . In other words, we wish to estimate the large t asymptotics of the probability $p(\mathcal{T}^0, \mathcal{T}_L^*; t)$ to grow a tree in t steps from some initial tree \mathcal{T}^0 (with left subtree \mathcal{T}_L^0) to a final state made of a *fixed final left subtree* \mathcal{T}_L^* of finite mass T_L^* and an arbitrary right subtree, necessarily with a large mass of order t . This probability clearly decays at large t and we expect a power law behavior of the form

$$p(\mathcal{T}^0, \mathcal{T}_L^*; t) \sim t^{-\gamma(\mathcal{T}^0, \mathcal{T}_L^*)} \quad (3.4)$$

The computation of the exponent $\gamma(\mathcal{T}^0, \mathcal{T}_L^*)$ will be a prerequisite for that of the mass distribution exponent β_L .

The probability $p(\mathcal{T}^0, \mathcal{T}_L^*; t)$ is the sum of the probabilities of all possible tree-growths of total size t leading from \mathcal{T}^0 to a tree with left subtree \mathcal{T}_L^* . It will prove convenient to divide any such process into a first initial sub-process evolving up to some fixed time t_0 and a later process from t_0 to t . The value of t_0 is kept finite but is chosen to be large enough so that the mean-field approximation can be applied to the (large enough) right subtree at each step of its evolution between t_0 and t . We may classify all processes according to the intermediate configuration $\mathcal{T}^{0'}$ attained at time t_0 . Note that $\mathcal{T}^{0'}$ necessarily has a left subtree $\mathcal{T}_L^{0'}$ intermediate between \mathcal{T}_L^0 and \mathcal{T}_L^* . This allows us to rewrite

$$p(\mathcal{T}^0, \mathcal{T}_L^*; t) = \sum_{\substack{\mathcal{T}^{0'} \\ \mathcal{T}_L^0 \subset \mathcal{T}_L^{0'} \subset \mathcal{T}_L^*}} \pi(\mathcal{T}^0, \mathcal{T}^{0'}; t_0) p(\mathcal{T}^{0'}, \mathcal{T}_L^*; t - t_0) \quad (3.5)$$

with some probabilities $\pi(\mathcal{T}^0, \mathcal{T}^{0'}; t_0)$ that correspond to the initial sub-process. These probabilities are a finite set of fixed positive numbers *independent of* t .

In turn, the second part of the process may be sorted according to the *induced* left-subtree growth process. The latter corresponds to the successive addition of links to the left subtree $\mathcal{T}_L^{0'}$ until we reach \mathcal{T}_L^* . We will denote by G_L such a left-subtree growth process, characterized by the sequence of trees leading from $\mathcal{T}_L^{0'}$ to \mathcal{T}_L^* . Beside the precise sequence of links added, we also need to specify the time t_j at which the j -th link is added, with j running from 1 to $J = T_L^* - T_L^{0'}$ (where $T_L^{0'}$ is the mass of $\mathcal{T}_L^{0'}$) and with $t_0 < t_1 < t_2 < \dots < t_J \leq t$. Between any two consecutive such times, the growth process only affects the right subtree. This allows us to rewrite

$$p(\mathcal{T}^{0'}, \mathcal{T}_L^*; t - t_0) = \sum_{G_L; t_1, t_2, \dots, t_J} p(G_L; t_1, t_2, \dots, t_J) \quad (3.6)$$

where the sum extends over all left-subtree growth processes G_L with fixed initial and final conditions as above, supplemented by the sequence of times t_j . The probability $p(G_L; t_1, \dots, t_J)$ of any given such process depends only on the sequence of the numbers $n_i^j \equiv n_{i,L}(t_j)$ of uni- and bi-valent vertices in the left subtree at time t_j (i.e., for $j \geq 1$, just after the addition of the j -th link). As before, we adopt the convention that $n_1^0 = 0$, $n_2^0 = 1$ when $\mathcal{T}_L^{0'}$ is empty. The probability $p(G_L; t_1, \dots, t_J)$ can be estimated as follows: from time t_j to time $t_{j+1} - 1$ (with the convention that $t_{J+1} = t$), the process only takes place on the right, hence has a probability

$$\prod_{\tau=t_j}^{t_{j+1}-1} \frac{n_{1,R}(\tau)w_1 + n_{2,R}(\tau)w_2}{(n_1^j + n_{1,R}(\tau))w_1 + (n_2^j + n_{2,R}(\tau))w_2} \sim \prod_{\tau=t_j}^{t_{j+1}-1} \left(1 + \frac{n_1^j w_1 + n_2^j w_2}{\alpha_1 w_1 + \alpha_2 w_2} \frac{1}{\tau} \right)^{-1} \quad (3.7)$$

where we have used the mean-field estimate $n_{i,R}(\tau) \sim \alpha_i \tau$ with α_i as in (2.7). At time $\tau = t_{j+1}$ ($0 \leq j \leq J - 1$), the process takes places on the left, hence has a probability

$\sim (n_1^j w_1 + n_2^j w_2) / ((\alpha_1 w_1 + \alpha_2 w_2) t_{j+1})$. This results in

$$p(G_L; t_1, \dots, t_J) \sim \prod_{\tau=t_0}^{t_1-1} \left(1 + \frac{q_0}{\tau}\right)^{-1} \times \frac{q_0}{t_1} \times \prod_{\tau=t_1}^{t_2-1} \left(1 + \frac{q_1}{\tau}\right)^{-1} \times \frac{q_1}{t_2} \times \dots \times \frac{q_{J-1}}{t_J} \times \prod_{\tau=t_J}^{t-1} \left(1 + \frac{q_J}{\tau}\right)^{-1} \quad (3.8)$$

where we have used the notation

$$q_j \equiv \frac{n_1^j w_1 + n_2^j w_2}{\alpha_1 w_1 + \alpha_2 w_2} \quad (3.9)$$

We may now fix the left-subtree growth process G_L , i.e. keep the *same* sequence of link additions, but sum over the times t_j , resulting in a probability $p(G_L)$ such that

$$p(\mathcal{T}^{0'}, \mathcal{T}_L^*; t - t_0) = \sum_{G_L} p(G_L) \quad (3.10)$$

The corresponding nested sums over intermediate times are further approximated by nested integrals, with the result

$$p(G_L) \sim \int_{t_0 < t_1 < \dots < t_J < t} \left(\prod_{j=1}^J \frac{dt_j}{t_j} q_{j-1} \left(\frac{t_{j-1}}{t_j} \right)^{q_{j-1}} \right) \left(\frac{t_J}{t} \right)^{q_J} = \sum_{j=0}^J \frac{q_j}{q_J} \left(\frac{t_0}{t} \right)^{q_j} \prod_{\substack{i=0 \\ i \neq j}}^J \frac{q_i}{q_i - q_j} \quad (3.11)$$

Again the precision of this latest approximation is governed by the choice of t_0 , and can be arbitrarily accurate by picking a large enough t_0 . The large t behavior of $p(G_L)$ therefore reads

$$p(G_L) \sim t^{-\gamma} \quad \text{where} \quad \gamma = - \min_{j \in \{0, 1, \dots, J\}} q_j. \quad (3.12)$$

Introducing the notation

$$q(\mathcal{T}) \equiv \frac{n_1(\mathcal{T})w_1 + n_2(\mathcal{T})w_2}{\alpha_1 w_1 + \alpha_2 w_2} \quad (3.13)$$

for any tree \mathcal{T} with $n_i(\mathcal{T})$ i -valent vertices, the minimum in (3.12) is equivalently obtained as the minimum of $q(\mathcal{T})$ when \mathcal{T} runs over all the intermediate trees of the growth process G_L , namely

$$p(G_L) \sim t^{-\min_{\mathcal{T} \in G_L} q(\mathcal{T})}. \quad (3.14)$$

Returning to $p(\mathcal{T}^{0'}, \mathcal{T}_L^*; t - t_0)$, we read from the summation in eq. (3.10) that

$$p(\mathcal{T}^{0'}, \mathcal{T}_L^*, t - t_0) \sim t^{-\min_{\mathcal{T}^{0'} \subset \mathcal{T} \subset \mathcal{T}_L^*} q(\mathcal{T})} \quad (3.15)$$

with the minimum now taken over all trees intermediate between $\mathcal{T}_L^{0'}$ and \mathcal{T}_L^* . Finally, from eq. (3.5), we have to sum over all possible trees $\mathcal{T}^{0'}$ at time t_0 , extending the range

of trees in the minimum to all trees intermediate between \mathcal{T}_L^0 and \mathcal{T}_L^* . This results in a behavior $p(\mathcal{T}^0, \mathcal{T}_L^*; t) \sim t^{-\gamma(\mathcal{T}^0, \mathcal{T}_L^*)}$ with

$$\gamma(\mathcal{T}^0, \mathcal{T}_L^*) = \min_{\mathcal{T}_L^0 \subset \mathcal{T} \subset \mathcal{T}_L^*} q(\mathcal{T}) \quad (3.16)$$

In practice, the exponent $\gamma(\mathcal{T}^0, \mathcal{T}_L^*)$ depends only weakly on \mathcal{T}_L^* . It proves useful to define a *generic* exponent

$$\gamma(\mathcal{T}^0) \equiv \min_{\mathcal{T}_L^0 \subset \mathcal{T}} q(\mathcal{T}) \quad (3.17)$$

with no upper bound on \mathcal{T} . In view of the discussion of section 3.1, the minimum is reached for some finite tree \mathcal{T}_{\min} (with $\mathcal{T}_{\min} = \mathcal{T}_L^0$ if $w_1 > w_2$ while, when $w_2 > w_1$, $\mathcal{T}_{\min} = \mathcal{S}_L^0$, the tree obtained by saturating each bivalent vertex of \mathcal{T}_L^0 into a trivalent vertex). We immediately deduce that $\gamma(\mathcal{T}^0, \mathcal{T}_L^*)$ takes the generic value $\gamma(\mathcal{T}^0)$ as soon as \mathcal{T}_L^* contains \mathcal{T}_{\min} . Moreover, if this is not the case, we necessarily have $\gamma(\mathcal{T}^0, \mathcal{T}_L^*) \geq \gamma(\mathcal{T}^0)$.

3.3. Scaling argument

The left exponent β_L can be obtained from the exponent $\gamma(\mathcal{T}^0)$ via a simple scaling argument. Indeed the distribution $P(u_L, u_R)$ for the left/right distribution of the mass is obtained as

$$P(u_L, u_R) = \lim_{t \rightarrow \infty} t^2 p(u_L(t + T^0 - 1), u_R(t + T^0 - 1); t) \quad (3.18)$$

where $p(T_L, T_R; t)$ is the probability to have reached after t steps left and right masses T_L and T_R respectively. This probability implicitly depends on the initial condition \mathcal{T}^0 (of total mass T^0). We have of course $T_L + T_R = t + T^0 - 1$ hence we may write

$$p(T_L, T_R; t) = p(T_L; t) \delta_{T_L + T_R, t + T^0 - 1} \quad (3.19)$$

as well as

$$P(u_L, u_R) = P(u_L) \delta(u_R + u_L - 1) \quad (3.20)$$

where the two reduced functions are now related through

$$P(u_L) = \lim_{t \rightarrow \infty} t p(u_L(t + T^0 - 1); t) \quad (3.21)$$

The exponent β_L characterizes the behavior of $P(u_L)$ at small u_L via

$$P(u_L) \sim u_L^{\beta_L} \quad \text{when } u_L \rightarrow 0 \quad (3.22)$$

At large t and for large but finite T_L , we may according to (3.21) and (3.22) estimate $p(T_L; t)$ via

$$p(T_L; t) \sim \frac{1}{t} P\left(\frac{T_L}{t}\right) \sim \frac{1}{t} \left(\frac{T_L}{t}\right)^{\beta_L} \quad (3.23)$$

hence $p(T_L; t)$ has a power law decay $t^{-(\beta_L+1)}$. The above estimate holds in the range $1 \ll T_L \ll t$. The probability $p(T_L; t)$ is the sum of the probabilities $p(\mathcal{T}^0, \mathcal{T}_L^*; t)$ over all final left subtree \mathcal{T}_L^* of mass T_L . From the results of previous section, each $p(\mathcal{T}^0, \mathcal{T}_L^*; t)$ decays as $t^{-\gamma(\mathcal{T}^0, \mathcal{T}_L^*)}$ and, as T_L is large enough, some of the \mathcal{T}_L^* 's will reach the (dominant) generic value $\gamma(\mathcal{T}^0)$. We deduce that

$$\beta_L + 1 = \gamma(\mathcal{T}^0) \quad (3.24)$$

with $\gamma(\mathcal{T}^0)$ given by (3.17). Hence, the announced result (3.1).

3.4. Numerical checks

To corroborate the above results, we have made a number of numerical checks. Those are based on random generation of large time Markov processes according to (2.1) or its left/right refinement. All simulations are made of growth processes with $t = 4000$ steps. The number N of runs ranges from 2×10^5 to 10^8 according to the desired precision and various values of $x = 2w_2/w_1$ are explored.

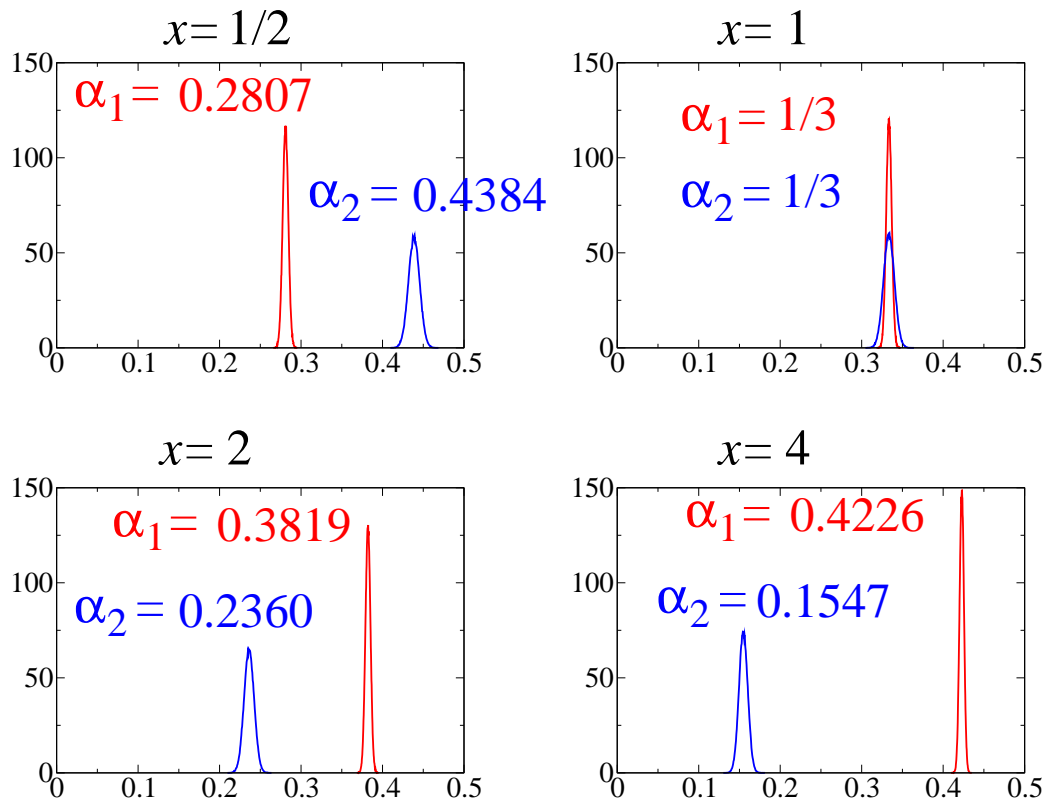


Fig. 6: The measured distribution (see text) for n_1/t (red) and n_2/t (blue) and the corresponding mean-field predictions from (2.7).

The first test concerns the distribution of the ratios n_i/t ($i = 1, 2$), to be compared with the results of section 2.2. Figure 6 displays the measured distribution obtained from $N = 2 \times 10^5$ runs with an initial tree reduced to the root edge, and for $x = 1/2, 1, 2$ and 4. As expected, we observe distributions peaked around precise values α_1 and α_2 corroborating the mean field predictions (2.7). The distributions and their widths agree perfectly with the Gaussian shape (2.13) and its α_2 counterpart.

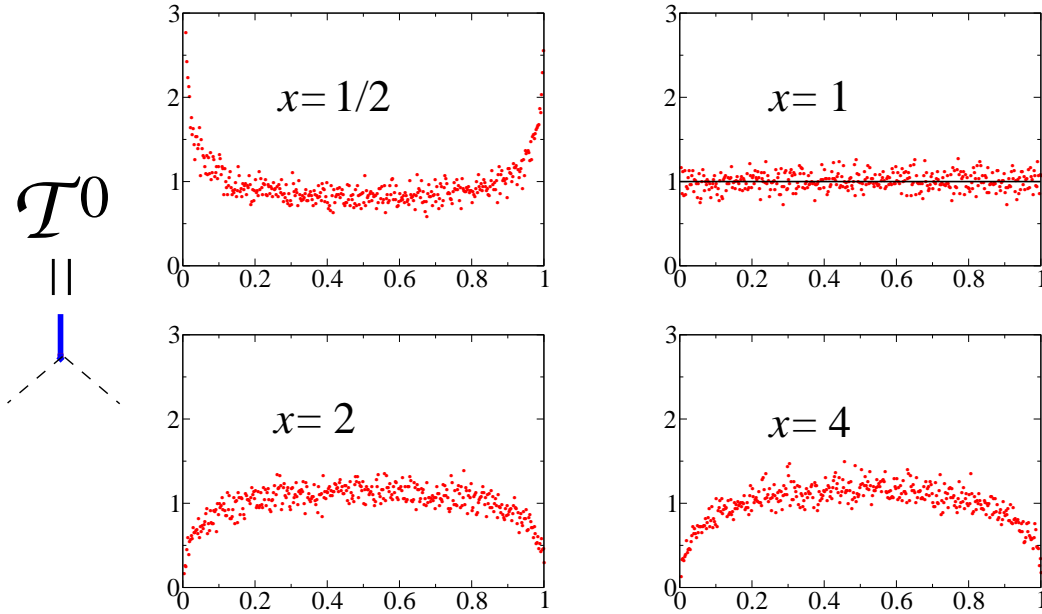


Fig. 7: Measured distribution $P(u_L)$ for the initial tree \mathcal{T}^0 drawn on the left. For $x = 1$, we have also indicated the exact distribution.

Next, we have explored the left/right mass distribution for various initial conditions and various of x . Again the statistics is over $N = 2 \times 10^5$ runs and we have chosen the values $x = 1/2, 1, 2$ and 4. Figures 7-10 show the measured distribution $P(u_L)$ of the proportion u_L of the total mass lying on the left side. Each point corresponds to an average over 10 consecutive values of the left mass, with $t/10 = 400$ such points. The initial configurations are (i) the tree reduced to the root edge (figure 7), (ii) the tree reduced to root edge and its left descendant (figure 8), (iii) the tree reduced to root edge and its two descendants (figure 9) and (iv) the tree reduced to root edge and a chain of length 2 on the left (figure 10). For $x = 1$, we have also indicated the exact limiting distribution as obtained by integrating (2.18) over u_R .

The very same data give access to the *integrated* distribution

$$D(u_L) \equiv \int_0^{u_L} P(u) du \quad (3.25)$$

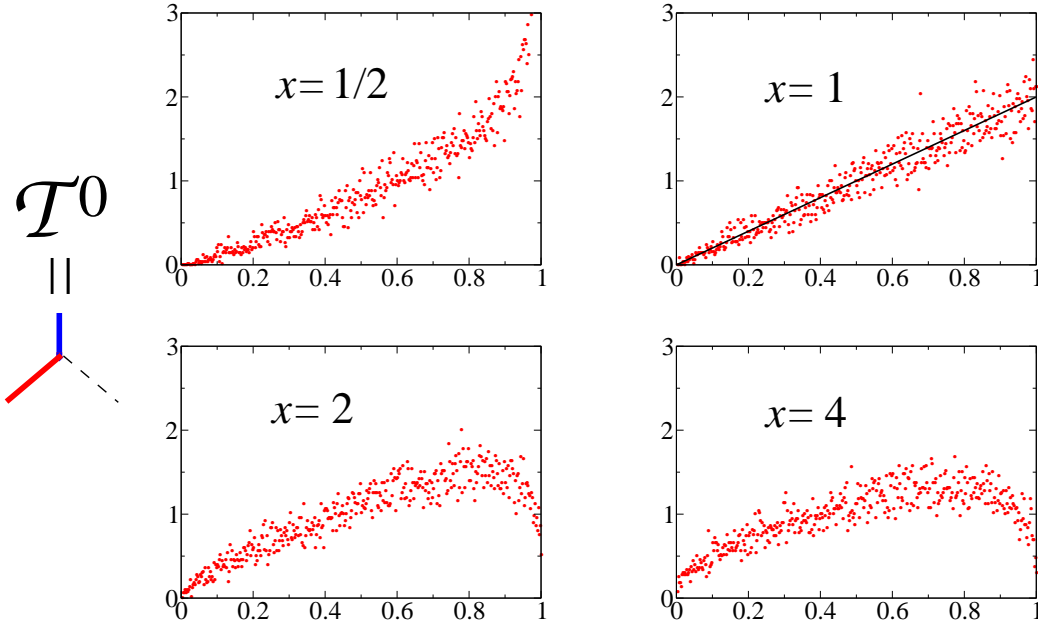


Fig. 8: Measured distribution $P(u_L)$ for the initial tree \mathcal{T}^0 drawn on the left.

by a simple cumulative sum. This wipes out the fluctuations of $P(u)$, leading to smoother curves displayed in figure 11. In this representation, the measured $x = 1$ curves are indistinguishable from their exact values deduced from (2.18).

We now come to a check of the prediction (3.16) for the exponent $\gamma(\mathcal{T}^0, \mathcal{T}_L^*)$ governing the t decay of the probability $p(\mathcal{T}^0, \mathcal{T}_L^*; t)$ to go in t steps from an initial tree \mathcal{T}^0 to a large final tree with left part \mathcal{T}_L^* . The predicted exponents (3.16) are plotted against their measured values, i.e. the limiting slopes of a log-log plot of the probability $p(\mathcal{T}^0, \mathcal{T}_L^*; t)$ versus t . The plots 12 and 13 have been obtained from a statistics over $N = 10^8$ runs for $x = 1/2$ and $x = 4$ and starting with the initial tree \mathcal{T}^0 indicated. The various curves correspond to various final left configurations \mathcal{T}_L^* as indicated in medallions. For $x = 1/2$, all curves display the same exponent compatible with the predicted value (3.17) for the generic exponent $\gamma(\mathcal{T}^0)$. Indeed, in this case, the minimum in (3.16) is always attained for the initial tree \mathcal{T}^0 irrespectively of \mathcal{T}_L^* . This is generic of all values $x < 2$. For $x = 4$, we see two distinct slopes according to whether \mathcal{T}_L^* contains or not the left subtree \mathcal{S}_L^0 obtained by saturating the initial left subtree \mathcal{T}_L^0 (see section 3.2). If it does, we observe the generic value $\gamma(\mathcal{T}^0)$ (3.17) and if not, we observe the larger value $\gamma(\mathcal{T}^0, \mathcal{T}_L^0)$ (3.16).

Finally, we have made a direct measurement of the left exponent β_L from the small u_L behavior (3.22) of $P(u_L)$. The statistics is over $N = 10^7$ runs for an initial tree \mathcal{T}^0 made of the root edge and its two descendants. The results are gathered in fig.14 in a log-log plot of $P(u_L)$ versus u_L for the values $x = 1/2, 1, 2, 4$ and 12. Each point

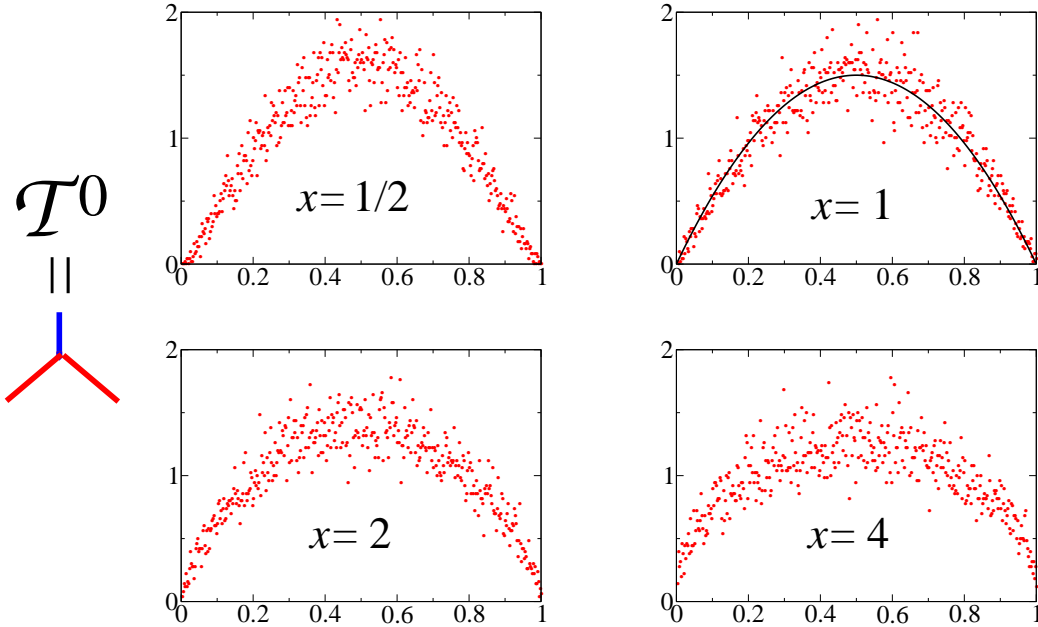


Fig. 9: Measured distribution $P(u_L)$ for the initial tree \mathcal{T}^0 drawn on the left.

corresponds to a left mass ranging from 1 to 100 over a total mass of 4000, hence u_L ranges from 0 to .025. The predicted slopes β_L are indicated by straight lines, with a perfect agreement in the range of large enough masses (here larger than 30), as expected from the scaling argument of section 3.3. For large x , we observe a parity effect due to the fact that the large x preferred value $n_{2,L} = 0$ (saturated tree) can be attained only for odd left masses. For $x = 12$, we have also represented the average between two consecutive left masses so as to wipe out this parity effect (empty green diamonds). This seems to extend the range of validity of the scaling argument to lower u_L 's.

The very same data are used in fig.15 to construct the log-log plot of the integrated distribution $D(u_L)$ (3.25) versus u_L by simple cumulative sums. This wipes out the statistical fluctuations of the previous plot and the results corroborate unambiguously our predictions for β_L .

4. Growth of multinary trees

4.1. Definition of the model

In this section, we generalize our results to trees with vertex valences up to $k+1$ for some fixed integer $k \geq 2$. As before, the trees are planar and rooted and may be thought of as drawn on top of an underlying $(k+1)$ -valent Cayley tree with a unique leaf attached to the root edge. We start from some initial finite tree \mathcal{T}^0 containing the root edge and add iteratively links at vertices with valence i less or equal to k , with probability weights

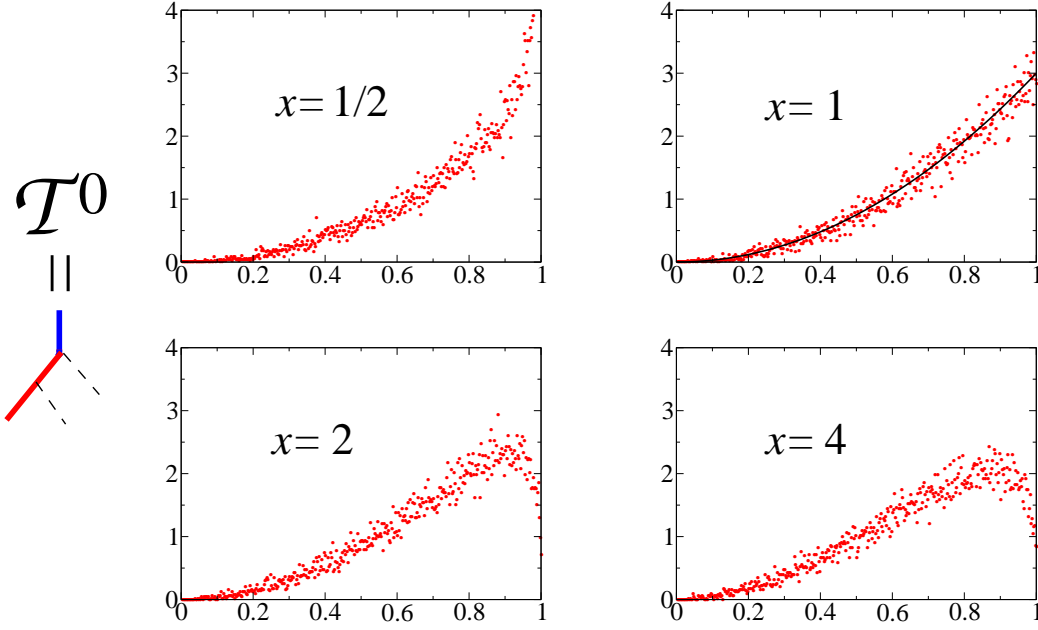


Fig. 10: Measured distribution $P(u_L)$ for the initial tree \mathcal{T}^0 drawn on the left.

w_i , $i = 1, \dots, k$. More precisely, if the tree has n_j j -valent vertices ($j = 1, \dots, k+1$), a given vertex of valence i is chosen with probability $w_i / (\sum_{j=1}^k n_j w_j)$. Once the vertex is chosen, the choice of link to add is uniformly distributed on all the $(k+1-i)$ available descendant edges. Again, this growing process induces a Markovian evolution for the numbers $n_i(t)$ of i -valent vertices at time step t starting from $n_i(0) \equiv n_i^0$, the numbers of i -valent vertices on \mathcal{T}^0 . We have the evolution rules

$$\begin{aligned}
 & \text{with probability } \frac{n_1(t)w_1}{\sum_{j=1}^k n_j(t)w_j}, \quad \begin{cases} n_1(t+1) &= n_1(t) \\ n_2(t+1) &= n_2(t) + 1 \\ n_\ell(t+1) &= n_\ell(t), \quad \ell \geq 3 \end{cases} \\
 & \text{with probability } \frac{n_i(t)w_i}{\sum_{j=1}^k n_j(t)w_j}, \quad \begin{cases} n_1(t+1) &= n_1(t) + 1 \\ n_i(t+1) &= n_i(t) - 1 \\ n_{i+1}(t+1) &= n_{i+1}(t) + 1 \\ n_\ell(t+1) &= n_\ell(t), \quad \ell \neq 1, i, i+1 \end{cases}
 \end{aligned} \tag{4.1}$$

for $i = 2, \dots, k$.

As before, we shall be interested in the repartition of the total mass T (number of edges) of the growing tree between the k descending subtrees of the root edge. If we denote by T_m the mass of the m -th descendant subtree from the left (with $T =$

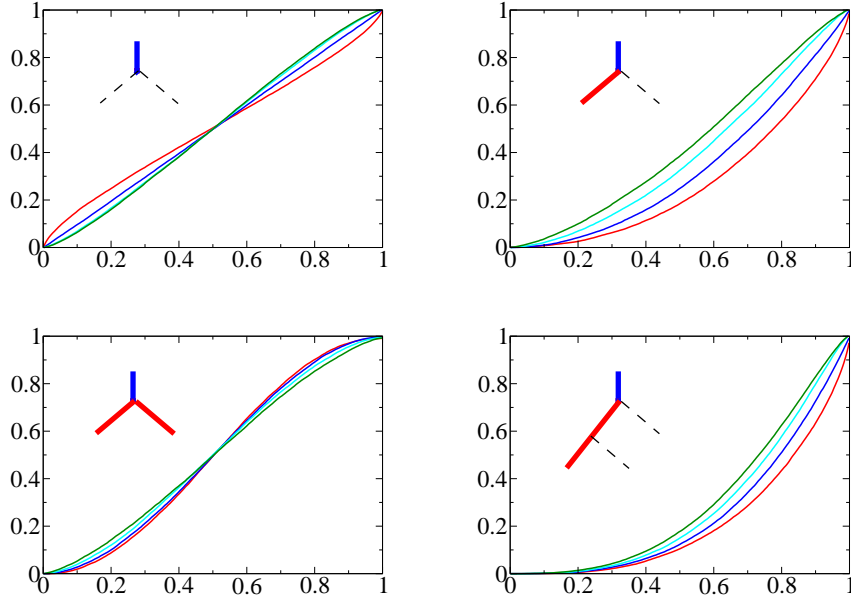


Fig. 11: Measured integrated distributions $D(u)$ for $x = 1/2$ (red), $x = 1$ (blue), $x = 2$ (cyan) and $x = 4$ (green) and for the four initial conditions indicated.

$1 + \sum_m T_m$), and $u_m \equiv T_m / (T - 1)$, we expect a broad limiting distribution $P(u_1, \dots, u_k)$ at large T characterized by mass distribution exponents β_m such that

$$P(u_1, \dots, u_k) \sim u_m^{\beta_m} \quad \text{when } u_m \rightarrow 0 \quad (4.2)$$

4.2. Mean field

As for binary trees, the expression for the mass distribution exponents β_m involves the limiting proportions α_i of i -valent vertices in trees grown for a long time t . Those are again exactly given by a set of mean field equations

$$\begin{aligned} \alpha_1 &= 1 - \frac{\alpha_1 w_1}{\Sigma} \\ \alpha_i &= \frac{\alpha_{i-1} w_{i-1} - \alpha_i w_i}{\Sigma}, \quad i = 2, \dots, k \end{aligned} \quad (4.3)$$

where we have defined $\Sigma = \sum_{i=1}^k \alpha_i w_i$. These equations are easily solved into

$$\alpha_i = \frac{\Sigma}{w_i} \prod_{j=1}^i \frac{w_j}{\Sigma + w_j} \quad (4.4)$$

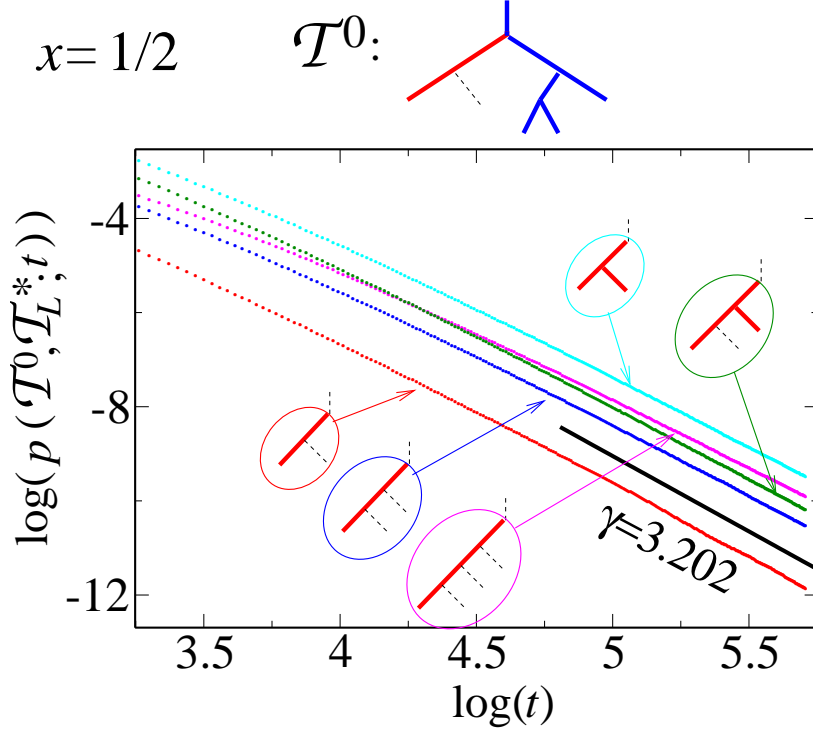


Fig. 12: Measured exponents $\gamma(\mathcal{T}^0, \mathcal{T}_L^*)$ at $x = 1/2$ from (minus) the slope of $p(\mathcal{T}^0, \mathcal{T}_L^*; t)$ vs t in a log-log plot, for an initial tree \mathcal{T}^0 as indicated and for various final left subtrees as shown in medallions. The black segment corresponds to the predicted exponent, here independent on \mathcal{T}_L^* .

where Σ is determined by the consistency equation $\Sigma = \sum_{i=1}^k \alpha_i w_i$, namely

$$f(\Sigma) \equiv \sum_{i=1}^k \prod_{j=1}^i \frac{w_j}{\Sigma + w_j} = 1 \quad (4.5)$$

Note that the function $f(\Sigma)$ is strictly decreasing from $f(0) = k$ to $f(\infty) = 0$, therefore eq. (4.5) has a unique real positive solution and the equation for the proportions (4.4) follow.

4.3. A solvable case

Here again, a particularly simple case corresponds to growing the trees by adding links chosen uniformly at random among all possible available positions. This amounts to taking $w_i = (k + 1 - i)$ in which case $\sum w_i n_i = (k - 1)T + 1$ directly counts the number of available positions for the addition of a link. In this case, we find $\Sigma = k - 1$ and the limiting proportions $\alpha_i = \binom{2k-i-1}{k-2} / \binom{2k-1}{k}$. Moreover, we can write a master equation for the probability $p(T_1, \dots, T_k; t)$ to have mass T_m for the m -th descendant

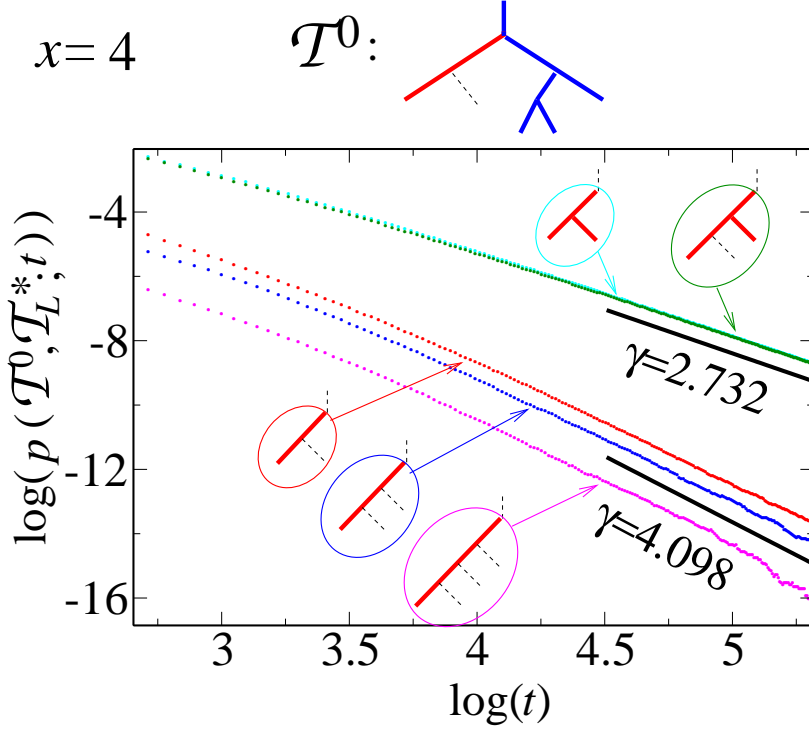


Fig. 13: Measured exponents $\gamma(\mathcal{T}^0, \mathcal{T}_L^*)$ at $x = 4$ from (minus) the slope of $p(\mathcal{T}^0, \mathcal{T}_L^*; t)$ vs t in a log-log plot, for an initial tree \mathcal{T}^0 as indicated and for various final left subtrees as shown in medallions. The black segment corresponds to the two predicted exponents, depending on \mathcal{T}_L^* (see text).

subtree from the left after t steps:

$$p(T_1, \dots, T_k; t+1) = \sum_{m=1}^k \frac{(k-1)(T_m-1)+1}{(k-1)(t+T^0)+1} p(T_1, \dots, T_{m-1}, T_m-1, T_{m+1}, \dots, T_k; t) \quad (4.6)$$

with initial condition $p(T_1, \dots, T_k; 0) = \prod_{m=1}^k \delta_{T_m, T_m^0}$. Note that this equation may alternatively be interpreted in terms of a generalized RRW in which a walker steps in one of k given directions labelled $m = 1, 2, \dots, k$ with a probability proportional to a function $f_m(N_m)$ of the number of times $N_m = T_m - T_m^0$ he already stepped in that direction. Here the functions read $f_m(N) = N + T_m^0 + 1/(k-1)$. In this language, $p(T_1, \dots, T_k; t)$ is the probability to have stepped $T_m - T_m^0$ times in the m -th direction after t steps (note that in this language T_m and T_m^0 need not be integers but N_m are). Eq.(4.6) is easily solved into

$$p(T_1, \dots, T_k; t) = \frac{t! \Gamma\left(T^0 + \frac{1}{k-1}\right)}{\Gamma\left(T^0 + t + \frac{1}{k-1}\right)} \prod_{m=1}^k \frac{\Gamma\left(T_m + \frac{1}{k-1}\right)}{(T_m - T_m^0)! \Gamma\left(T_m^0 + \frac{1}{k-1}\right)} \delta_{1 + \sum_m T_m, t + T^0} \quad (4.7)$$

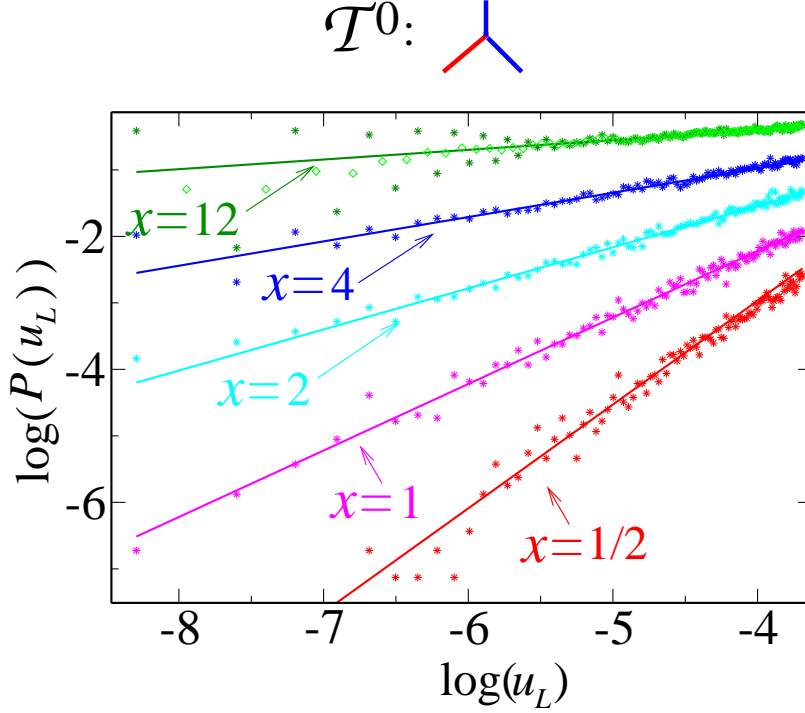


Fig. 14: Measured exponent β_L from the slope of $P(u_L)$ vs u_L in a log-log plot, for an initial tree \mathcal{T}^0 as indicated and for various values of x . The straight lines correspond to the predicted exponents.

which yields the limiting distribution $P(u_1, \dots, u_k) \equiv \lim_{t \rightarrow \infty} t^k p(\{u_m(t + T^0 - 1)\}; t)$:

$$P(u_1, \dots, u_k) = \frac{\Gamma\left(T^0 + \frac{1}{k-1}\right)}{\prod_{m=1}^k \Gamma\left(T_m^0 + \frac{1}{k-1}\right)} \prod_{m=1}^k u_m^{T_m^0 - \frac{k-2}{k-1}} \delta\left(\sum_{m=1}^k u_m - 1\right) \quad (4.8)$$

We can therefore read off the mass distribution exponents for this particular case:

$$\beta_m = T_m^0 - \frac{k-2}{k-1} \quad (4.9)$$

4.4. Mass distribution exponents

In the case of arbitrary weights w_j , the mass distribution exponents may be evaluated along the same lines as in Section 3, with the result

$$\beta_m = -1 + \frac{1}{\Sigma} \min_{\mathcal{T} \supset \mathcal{T}_m^0} \left\{ \sum_{j=1}^k w_j n_j(\mathcal{T}) \right\} \quad (4.10)$$

with Σ the solution of eq. (4.5) and where the minimum is taken over all trees \mathcal{T} containing the m -th initial subtree \mathcal{T}_m^0 . Again we use the convention that whenever \mathcal{T} is empty, we set $n_1(\mathcal{T}) = \dots = n_{k-1}(\mathcal{T}) = 0$ and $n_k(\mathcal{T}) = 1$.

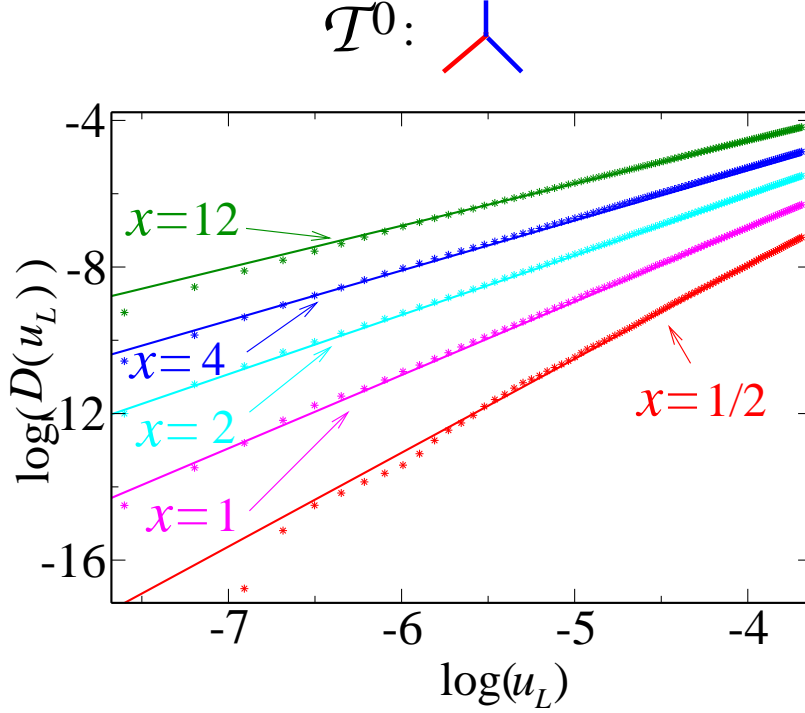


Fig. 15: Log-log plot of the integrated distribution $D(u_L)$ vs u_L from the same data as fig.14. The slope are now identified with $1 + \beta_L$, with a much better accuracy.

Note that, in the solvable case of previous section, the quantity to be minimized is simply $(k-1)T + 1$ where T is the mass of \mathcal{T} hence the minimum is reached for \mathcal{T}_m^0 , leading to the result $-1 + ((k-1)T_m^0 + 1)/\Sigma$, in agreement with eq. (4.9) as $\Sigma = k-1$.

For illustration, let us discuss the case $k=3$ in detail. It is convenient to view the trees \mathcal{T} as grown out of \mathcal{T}_m^0 and to follow the evolution of the quantity $r(\mathcal{T}) \equiv \sum_{j=1}^3 w_j n_j(\mathcal{T})$ that we wish to minimize. According to the evolution rules (4.1) applied to up to three consecutive steps, $r(\mathcal{T})$ has increments

$$\begin{aligned}
 & w_2 && \text{when attaching one link to a univalent vertex} \\
 & w_3 + w_1 && \text{when attaching two links to a univalent vertex} \\
 & 2w_1 && \text{when attaching three links to a univalent vertex} \\
 & w_3 + w_1 - w_2 && \text{when attaching one link to a bivalent vertex} \\
 & 2w_1 - w_2 && \text{when attaching two links to a bivalent vertex} \\
 & w_1 - w_3 && \text{when attaching one link to a trivalent vertex}
 \end{aligned} \tag{4.11}$$

In particular, the increment is always positive whenever we attach new links to an existing univalent vertex. Let us introduce the ratios

$$y \equiv \frac{w_2}{w_1}, \quad z \equiv \frac{w_3}{w_1} \tag{4.12}$$

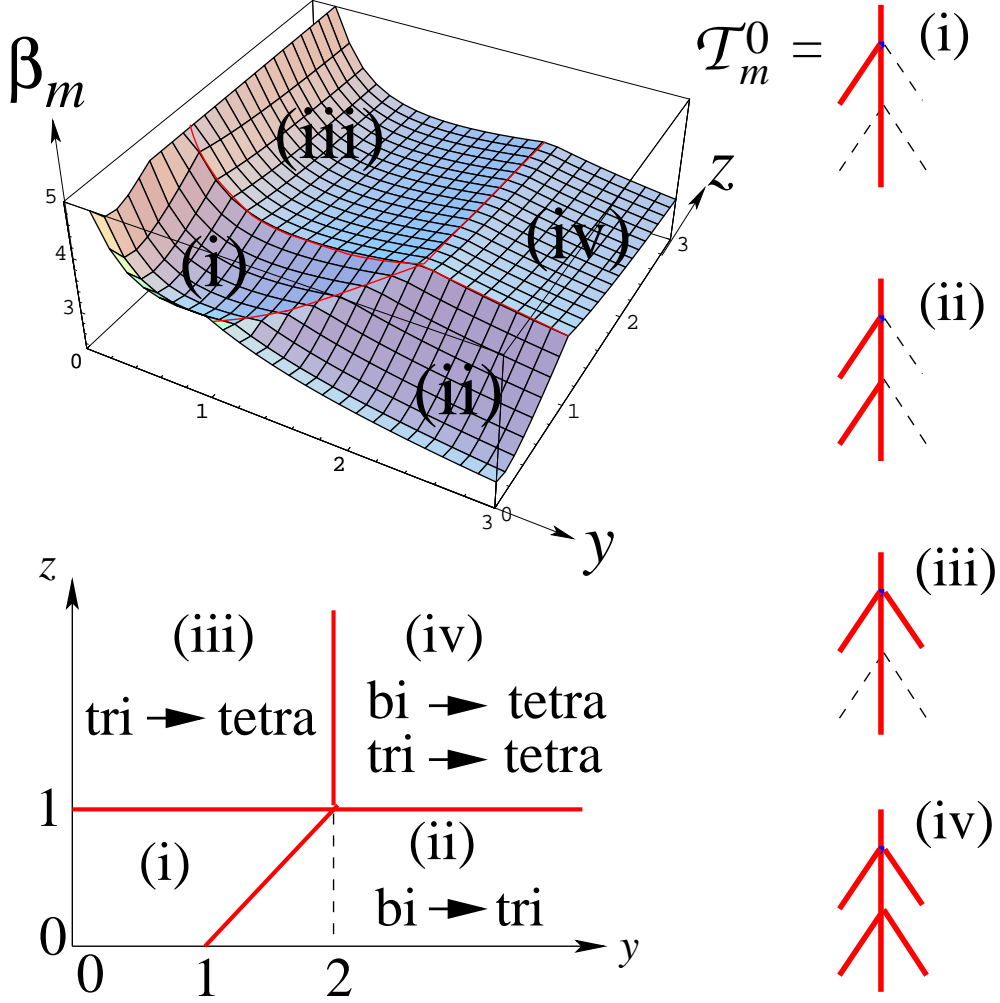


Fig. 16: The four regimes (i-iv) for the determination of the mass distribution exponent β_m in the $(y = w_2/w_1, z = w_3/w_1)$ plane. The exponent β_m is plotted here for the particular choice of \mathcal{T}_m^0 indicated in the upper right corner. We may always write $\beta_m = -1 + (n_1 w_1 + n_2 w_2 + n_3 w_3)/\Sigma$ provided we choose for n_i the number of i -valent vertices of the appropriate tree, namely: (i) the initial tree \mathcal{T}_m^0 , or (ii) a tree obtained from \mathcal{T}_m^0 by changing its bivalent vertices into trivalent ones, or (iii) the tree obtained from \mathcal{T}_m^0 by changing its trivalent vertices into tetravalent ones, or (iv) the tree obtained from \mathcal{T}_m^0 by changing both its bi- and trivalent vertices into tetravalent ones. These trees are displayed on the right.

For $z < 1$ and $y < z + 1$ (regime (i)), all increments above are positive. The minimum is therefore attained for the initial configuration $\mathcal{T} = \mathcal{T}_m^0$, with $n_i(\mathcal{T}) = n_i^m$ the initial numbers of i -valent vertices in \mathcal{T}_m^0 . For $z < 1$ and $y > z + 1$ (regime (ii)), the quantity $r(\mathcal{T})$ is minimized by adding exactly one link to all bivalent vertices of \mathcal{T}_m^0 , thus changing them into trivalent ones. The resulting tree \mathcal{T} now has $n_1(\mathcal{T}) = n_1^m + n_2^m$, $n_2(\mathcal{T}) = 0$ and $n_3(\mathcal{T}) = n_2^m + n_3^m$. For $z > 1$, it becomes favorable to add one link to all trivalent

vertices, thus changing them all into tetravalent vertices. As for bivalent vertices, either $y < 2$ (and in particular $y < z + 1$) and we leave these vertices unchanged (regime (iii)), resulting in a tree with $n_1(\mathcal{T}) = n_1^m + n_3^m$, $n_2(\mathcal{T}) = n_2^m$ and $n_3(\mathcal{T}) = 0$, or $y > 2$ and we must change these bivalent vertices into tetravalent ones (regime (iv)), resulting in a tree with $n_1(\mathcal{T}) = n_1^m + 2n_2^m + n_3^m$, $n_2(\mathcal{T}) = n_3(\mathcal{T}) = 0$. This allows us to write

$$\begin{aligned}
\text{(i)} \quad \beta_m &= \frac{n_1^m w_1 + n_2^m w_2 + n_3^m w_3}{\Sigma} - 1 \quad \text{for } z < 1, y < z + 1 \\
\text{(ii)} \quad \beta_m &= \frac{(n_1^m + n_2^m)w_1 + (n_2^m + n_3^m)w_3}{\Sigma} - 1 \quad \text{for } z < 1, y > z + 1 \\
\text{(iii)} \quad \beta_m &= \frac{(n_1^m + n_3^m)w_1 + n_2^m w_2}{\Sigma} - 1 \quad \text{for } z > 1, y < 2 \\
\text{(iv)} \quad \beta_m &= \frac{(n_1^m + 2n_2^m + n_3^m)w_1}{\Sigma} - 1 \quad \text{for } z > 1, y > 2
\end{aligned} \tag{4.13}$$

These formulae also hold whenever \mathcal{T}_m^0 is empty by setting $n_1^m = n_2^m = 0$ and $n_3^m = 1$. These results are summarized in figure 16 where the different regimes are displayed. We have also performed a number of numerical checks identical to those presented in section 3 and which fully corroborate the above results.

5. Conclusion

In this paper, we have derived the exact expression of exponents characterizing the mass distribution of trees growing locally by addition of links. As opposed to generic random trees whose statistics is governed by local Boltzmann weights, the mass of large growing trees is not in general concentrated in a single side of the root but can be distributed in all subtrees. The mass can be preferentially concentrated in one subtree (negative mass distribution exponent), it can be preferentially equally distributed over all subtrees (positive exponent) or it can be characterized by a uniform distribution (vanishing exponent). In practice, the precise value of the mass distribution exponent depends both on the growth process parameters w_i and on the initial condition \mathcal{T}^0 . In particular, in the case of binary trees grown from a single edge, the exponent β_L increases with x up to the transition point $x = 2$ and then decreases down to 0 at $x \rightarrow \infty$. This shows that a monotonous variation of the relative strength that we attach to the two types of vertices (univalent or bivalent) does not induce a monotonous variation of the characteristics of the tree.

We have observed that, except for special values of x where the model is exactly solvable, the mass distribution is not in general a Beta law and we may wonder whether an explicit analytic expression could be found. In this respect, a promising direction of investigation is provided by the approach of the problem via continuous time branching processes [8-10]. Indeed, within this framework, it is possible to relate the mass distribution to other asymptotic large time distributions which are themselves determined by coupled integral equations. Solving these equations analytically would be a major advance in this field.

For more general tree valences, an interesting outcome of our study is the existence of different regimes for the value of the mass distribution exponents. This seems to indicate the existence of a competition between various coexisting effective growth mechanisms. Whether the transitions between these regimes are characterized or not by the emergence of some order parameter remains to be understood.

Acknowledgments: We thank J. Bouttier for helpful discussions. All authors acknowledge support from the Programme d'Action Intégrée J. Verne “Physical applications of random graph theory” and from the ENRAGE European network, MRTN-CT-2004-5616. We acknowledge support from the Geocomp project, ACI Masse de données (P.D.F and E.G.), from the ENIGMA European network, MRTN-CT-2004-5652 (P.D.F) and from the ANR program GIMP, ANR-05-BLAN-0029-01 (F.D. and P.D.F.).

References

- [1] J. Ambjørn, B. Durhuus and T. Jonsson, *Quantum geometry: a statistical field theory approach*, Cambridge University Press, Cambridge (1997).
- [2] J. Ambjørn and R. Loll, *Non-perturbative Lorentzian Quantum Gravity, Causality and Topology Change*, Nucl. Phys. **B536** [FS] (1998) 407, hep-th/9805108.
- [3] P. Di Francesco and E. Guitter, *Critical and Multicritical Semi-Random $(1 + d)$ -Dimensional Lattices and Hard Objects in d Dimensions*, J.Phys. A35 (2002) 897-928.
- [4] R. Albert and A.-L. Barabási, *Statistical mechanics of complex networks*, Rev. Mod. Phys. **74** (2002) 47-97.
- [5] B. Durhuus, T. Jonsson and J. F. Wheeler, *The spectral dimension of generic trees*, [math-ph/0607020].
- [6] B. Durhuus, *Probabilistic aspects of infinite trees and surfaces*, Act. Phys. Pol. **34** (2003) 4795-4811.
- [7] see R. Pemantle, *A survey of random processes with reinforcement* and references therein, [math.PR/0610076].
- [8] S. Janson, *Functional limit theorems for multitype branching processes and generalized Pólya urns*, Stochastic Processes and their Applications **110** (2004) 177-245.
- [9] M. Drmota, S. Janson and R. Neininger, *A functional limit theorem for the profile of search trees*, [math.PR/0609385].
- [10] A. Rudas, B. Toth and B. Valko, *Random trees and general branching processes*, [math.PR/0503728].